Model. Earth Syst. Environ. (2016) 2:130
DOI 10.1007/s40808-016-0185-8

ORIGINAL ARTICLE

Modeling of soil exchangeable sodium percentage using easily obtained indices and artificial intelligence-based models

Ali Keshavarzi[1] · Ali Bagherzadeh[3] · El-Sayed Ewis Omran[2] · Munawar Iqbal[4,5]

Received: 26 June 2016 / Accepted: 4 July 2016 / Published online: 15 July 2016

Abstract Salinization and alkalization of land resources are the major obstacles to their optimal usage in many arid and semi-arid regions of the world, including Iran, since potential evapotranspiration is more noteworthy than precipitation in these areas. The amount of water that enters the soil is low and this results in salt accumulation in soils, which makes the soil infertile. Moreover, existence of salts, for example, sodium, in soils causes dispersion of soil particles and soil degradation, and intensifies soil erosion too. Monitoring exchangeable sodium percentage (ESP) variability in soils is both time-consuming and costly. However, in order to estimate the amounts of amendments and land management, it is necessary to know ESP variation and values in sodic or saline and sodic soils. Thus, introducing a method, which utilizes easily obtained indices to estimate ESP indirectly is more optimized and economical. Input and output data, i.e., EC_e (dS m^{-1}), clay (%), pH and ESP (%) were collected and measured from 100 soil samples in light of a stratified random sampling from Mashhad Plain, Khorasan-e-Razavi Province, Northeast Iran. This study aims to propose some models to estimate ESP by easily obtained properties of soil. In this regard, the efficiency of artificial intelligence-based (AI) models (i.e., Artificial Neural Network, ANN, and Adaptive Neuro-Fuzzy Inference System, ANFIS) was investigated and compared. Accuracy results showed that owing to highest R^2 and the lowest mean square error (MSE), ANFIS model predictions were superior to the MLP model for indirect estimation of soil exchangeable sodium percentage.

Keywords Artificial intelligence · Prediction · Exchangeable sodium percentage · Mashhad plain · Iran

Introduction

Precision agriculture practices in arid and semi-arid areas like Iran require periodic information on soil salinity and alkalinity, which are the most essential issues threatening sustainable agricultural management (Keshavarzi and Sarmadian 2012; Kilic and Kilic 2007; Omran 2008). The amount of agricultural lands having salinity and alkalinity problems increase continuously as identified with climate, topography, groundwater level and quality of irrigation water (Postel 1989; Ayers and Westcot 1989; Kilic and Kilic 2007). The most widely recognized reasons of salinity and alkalinity are low precipitation, high evapotranspiration, and low quality of irrigation water. Saline soils contain soluble salts in adequate amounts to interfere the growth of most crop plants, yet they do not contain enough exchangeable sodium to adjust soil characteristics (Kilic and Kilic 2007). However, alkali soils incorporate exchangeable sodium in a sufficient quantity to interfere with the growth of most crops (Bohn et al. 1985).

✉ Ali Keshavarzi
alikeshavarzi@ut.ac.ir

[1] Laboratory of Remote Sensing and GIS, Department of Soil Science, University of Tehran, P.O.Box: 4111, Karaj 31587-77871, Iran

[2] Soil and Water Department, Faculty of Agriculture, Suez Canal University, 41522 Ismailia, Egypt

[3] Department of Agriculture, Islamic Azad University, Mashhad Branch, Emamyeh Boulevard, P.O.Box: 91735-413, Mashhad, Iran

[4] Department of Chemistry, The University of Lahore, Raiwind Road, Lahore, Pakistan

[5] Department of Chemistry, Qurtuba University of Science and Information Technology, Peshawar, KPK 25100, Pakistan

Soluble salts influence the productivity of soils in two principal ways: changing the osmotic potential of soil solution and increasing the content of exchangeable sodium, which produces in many soils an unfavorable physical condition (Pozdnyakova and Zhang 1999). There is a close relationship between soil properties and salinity and alkalinity (Kilic and Kilic 2007), which is related to soil texture, water content and bulk density (Pozdnyakova and Zhang 1999). Salinity stress poses three challenges, including water shortage (drought stress), ionic toxicity, and nutrient imbalances to crops (Sarani et al. 2015). The presence of abundant ions in the root zone causes the absorption and effectiveness of nutrients to decrease greatly, and on the other hand, increases absorption of any unnecessary elements (Pessarakli 1991). Saline soils have increased significantly in Iran and throughout the world. Approximately 44.5 M ha of arable lands is influenced by dry land salinity in Iran (Banaei et al. 2005; Sarani et al. 2015). Moreover, the application of irrigation water of low quality may result in increasing soil salinity. Management of irrigated arid and semiarid soils and land application of industrial and food processing wastes often requires frequent monitoring of soil salinity and sodicity variation. Such monitoring practices are feasible and economical only where simple, straightforward, and rapid methods are accessible.

Despite the increasing prevalence of salinity worldwide, the estimation of exchangeable cation concentrations in saline soil remains problematic. In this situation, it is desirable to determine relationships among soil salinity indices. Soil electrical conductivity (EC), as a suitable index, which is reliable, cheap, and can be measured fast, has long been utilized by several researchers (Auerswald et al. 2001; Seilsepour and Rashidi 2008a; Adhikari et al. 2011). On the contrary, monitoring the changes of soil sodicity is costly in addition tedious. For saline or saline-sodic soils that are undergoing the amendment procedure, or when applying high sodium adsorption ratio (SAR) irrigation water or wastes, it is necessary to monitor the status of soil exchangeable sodium percentage (ESP) or SAR frequently. This, alongside pH and EC monitoring, is advisable for selecting and adjusting water and waste, estimating the amount of amendments and management practices (Robbins 1993). The SAR and ESP are two acknowledged indices for evaluating the degree of soil sodicity. The soil ESP is obtained by Eq. (1):

$$\mathrm{ESP} = \frac{Na_{\mathrm{exchangeable}}(me/100\mathrm{g\ soil})}{\mathrm{CEC}(me/100\mathrm{g\ soil})} \times 100 \qquad (1)$$

As shown in Eq. (1), determining the cation exchange capacity (CEC) is necessary for estimating soil ESP. The CEC measurement in the laboratory is very costly and time-consuming, and contains errors (Rashidi and Seilsepour 2008; Seilsepour and Rashidi 2008b, 2008c). In order to conquer the aforementioned issues, presenting a method that could utilize another parameter to calculate ESP in an indirect manner is more optimized and economical as well. Statistical methods have been widely used to model and predict the soil ESP from easily obtained indices. Robbins and Meyer (1990) predicted ESP from pH and EC in sodic and highly weathered soils of Australia and reported that this technique is economic, time-efficient, and potentially able to calculate ESP from pH and EC data. Farahmand et al. (2012) found nonlinear relationship in salt-affected soils of the Tabriz plain, Iran. Al-Busaidi and Cookson (2003) proposed an equation based on EC for saline soils in Oman. Sodicity is one of the properties of salt-affected soils and high values of exchangeable sodium are an indication of sodic soils.

Modeling ESP in the soil is important in numerous applications of soil science. Therefore, it is essential and inescapable to know ESP values in order to carry out suitable prevention measures and estimate the amounts of amendments for taking care this issue, which result in improving soil quality and sustainable agriculture development. Traditional determination methods which are lengthy, labor-intensive, and insufficiently accurate appear to be increasingly irrelevant to many users and does not have a market with land managers and policy makers (Omran 2008). A reliable and environmentally friendly method is needed to rapidly detect and analyze soil ESP. A growing demand for development of cost-effective methods for detecting and quantifying ESP in soil with reliable precision, lead us to a research objective, which aims to suggest some models to estimate ESP by easily obtained soil properties. In this regard, the efficiency of artificial intelligence-based models (i.e., Artificial Neural Network, ANN, and Adaptive Neuro-Fuzzy Inference System, ANFIS) was investigated and compared.

Materials and methods

Multi-layer perceptron (MLP)

A detailed background of ANN models can be found in Haykin (1999). However, in brief, ANNs composed of three distinct types of layers; one input layer, one or more hidden layers and one output layer. Each layer comprises of various straightforward processing elements called neurons or nodes. Data enters an ANN through the nodes of the input layer. The input layer nodes distribute the input information to the next layer (i.e., the first hidden layer). The hidden and output layer nodes process all incoming signals by applying factors to them (termed weights). Each layer also has an additional element called a bias. Bias

nodes simply output a signal to the nodes of the current layer. All inputs to a node are weighted, combined and then processed through a transfer function that controls the strength of the signal released through the node's output connections. Some of the most popular transfer (activation) functions are Sigmoid, Gaussian, Hyperbolic Tangent and Hyperbolic Secant (Malekmohammadi et al. 2011). Multilayer perceptron (MLP) is one of the commonly utilized ANN approaches for prediction studies. Figure 1 demonstrates the structure of an MLP neural network model. In this figure i, j and k denote input layer, hidden layer and output layer neurons, respectively, and w is the applied weight by the neuron. The gradient descent, conjugate gradient, Levenberg–Marquardt, etc. learning algorithms can be utilized for training the MLP model (Kisi et al. 2015; Barzegar and Asghari Moghaddam 2016). The explicit expression of an output value of a three-layered MLP is given by Nourani et al. (2013), Barzegar and Asghari Moghaddam (2016) and Barzegar et al. (2016b):

$$y_k = f_0\left[\sum_{i=1}^{M_N} W_{kj} f_h\left(\sum_{i=1}^{N_N} W_{ji}X_i + W_{j0}\right) + W_{k0}\right] \quad (2)$$

where, W_{ji} is a weight in the hidden layer connecting the ith neuron in the input layer and the jth neuron in the hidden layer, W_{j0} is the bias for the jth hidden neuron, f_h is the activation function of the hidden neuron, W_{kj} is a weight in the output layer connecting the jth neuron in the hidden layer and the kth neuron in the output layer, W_{k0} is the bias for the kth output neuron, f_0 is the activation function for the output neuron, X_i is ith input variable for input layer and y_j is computed output variable. N_N and M_N are the number of the neurons in the input and hidden layers, respectively.

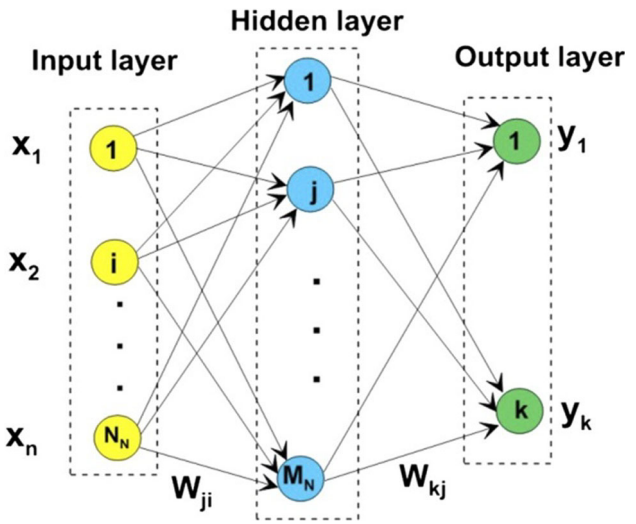

Fig. 1 Schematic diagram of a feed-forward MLP neural network (Barzegar and Asghari Moghaddam 2016)

Adaptive neuro-fuzzy inference system (ANFIS)

The adaptive neuro-fuzzy inference system (ANFIS) was introduced by Jang (1993) as a neural network functionally equivalent to a Sugeno type inference model. ANFIS utilizes a feed-forward network to search for fuzzy decision rules that perform well on a given task. Utilizing a given input–output data set, ANFIS creates a FIS for which membership function parameters are adjusted using either a back propagation algorithm alone or a combination of a back propagation algorithm and a least-squares method (Abdulshahed et al. 2015). This allows the fuzzy systems to learn from the data being modeled. The equivalent ANFIS architecture of the Sugeno inference system appears in Fig. 2. The entire system comprises of five layers, and the relationship between the input and output of each layer is summarized as follows (Barzegar and Asghari Moghaddam 2016):

Layer 1 Every node i in this layer is an adaptive node with a node output, O, defined by:

$$\begin{aligned} O_{1,i} &= \mu_{A_i}(x) \quad for\ i\ =\ 1,\ 2,\ or \\ O_{1,i} &= \mu_{B_{i-2}}(y) \quad for\ i\ =\ 3,\ 4 \end{aligned} \quad (3)$$

where, x (or y) is the input to the node, and A_i (or B_{i-2}) is a fuzzy set associated with this node, and characterized by the shape of the node's membership function (μ). This function must be continuous and piecewise differentiable, such as, for example, a Gaussian function. If such is used as a membership function, $\mu_{A_i}(x)$ can be computed as:

$$\mu_{A_i}(x) = e^{-\frac{1}{2}\left(\frac{x - C_i}{\sigma_i}\right)^2} \quad (4)$$

where, {σi, ci} are parameter sets.

Parameters in this layer are referred to as premise (antecedent) parameters.

Layer 2 Every node in this layer is a fixed node labeled as Π, which multiplies the incoming signals and output product. For instance,

$$O_{2,i} = w_i = \mu_{A_i}(x) \times \mu_{B_i}(y) \quad i = 1, 2 \quad (5)$$

with each output node representing the firing strength of a rule.

Layer 3 Every node in this layer is a circular node labeled as N. The ith node calculates the ratio of the ith rule's firing strength to the sum of all rules' firing strengths.

$$O_{3,i} = \bar{w} = \frac{w_i}{w_1 + w_2} \quad i = 1,\ 2 \quad (6)$$

This layer's outputs are termed normalized firing strengths.

Layer 4 Node i in this layer computes the contribution of the ith rule towards the model output, with the following node function:

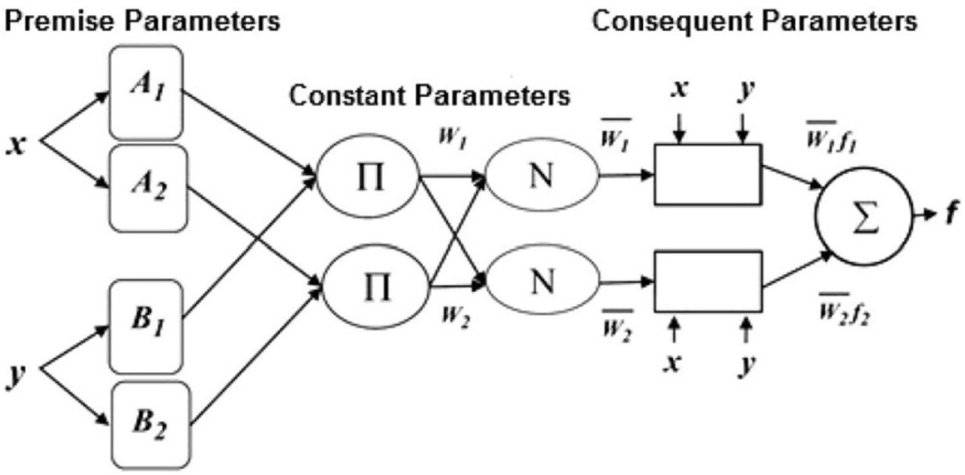

Fig. 2 A typical ANFIS architecture (Jang 1993)

$$O_{4,i} = \bar{w}_i f_i = \bar{w}_i(p_i x + q_i y + r_i) \tag{7}$$

where, w_i is the output of layer 3 and $\{p_i, q_i, r_i\}$ is the parameter set. Parameters in this layer are referred to as consequent parameters.

Layer 5 The single node in this layer is a fixed node, labeled Π that computes the overall output as the summation of all incoming signals.

$$O_{5,i} = \sum_{i=1}^{i=2} \bar{w}_i f_i = \frac{\sum_{i=1}^{i=2} w_i f_i}{\sum_{i=1}^{i=2} w_i} \tag{8}$$

Model performance criteria

The following statistical indicators were selected in the performance evaluation of constructed models (Barzegar et al. 2016c):

1. Coefficient of determination (R^2), and
2. Mean square error (MSE).

$$R^2 = \left[\sum_{i=1}^{N}(P_i - \bar{P})(O_i - \bar{O})\right]^2 \left[\sum_{i=1}^{N}(P_i - \bar{P})^2 (O_i - \bar{O})^2\right]^{-1} \tag{9}$$

$$MSE = \left[N^{-1}\sum_{i=1}^{N}(P_i - O_i)^2\right] \tag{10}$$

where, N is the number of observations, P_i is the predicted values, O_i is the observed data, and $P$and O are the mean values for P_i and O_i, respectively. The coefficient of determination (R^2) measures the degree of correlation among the observed and predicted values. R^2 values range from 0 to 1, with 1 indicating a perfect relationship between the data and the line drawn through them, while 0 represents no statistical correlation between the data and the line. The MSE evaluates the variance of errors independent of the sample size. MSE indicates the discrepancy between the observed and predicted values. A perfect fit between observed and predicted values would have an MSE of 0.

Site description

The present study was conducted in Mashhad Plain with an area of 6131 km^2, Khorasan-e-Razavi Province, Northeast Iran (Fig. 3). The study area is located between latitude 35°59′N to 37°04′N and longitude 58°22′E to 60°07′E. The general physiographic trend of the plain extends in a NW–SE direction with an average of 160 km in length surrounded by the two mountainous zones of Kopet-dagh northward and Binaloud southward based on a visual interpretation of the satellite imagery and field observations. The topographic elevation values of the study area vary between 900 and 1500 m.a.s.l., while the main topographical elevation ranges over 1200 m.a.s.l.

Geologically, the main alluvial nature of the plain has developed into a thick sediment-dominated environment belonging to the quaternary period. The main soil textures are loam, sandy loam and sandy clay loam. The dominant soil types include calcaric cambisols, gypsic regosols, calcaric regosols and calcaric fluvisols, which cover pediment plains, plateau and upper terraces and gravelly colluvial fans, respectively. The study area consisted of six cities with a population of about 2,481,290 and 519 villages with a population of about 422,610, scattered over the plain. The main land use practiced in the study area is irrigated farming around the Kashfrod River, with a semi-arid climate, mean annual precipitation of 222.1 mm and mean annual temperature of 15.8 °C. The rainiest month is March (44.8 mm) and the driest month is September (1.2 mm).

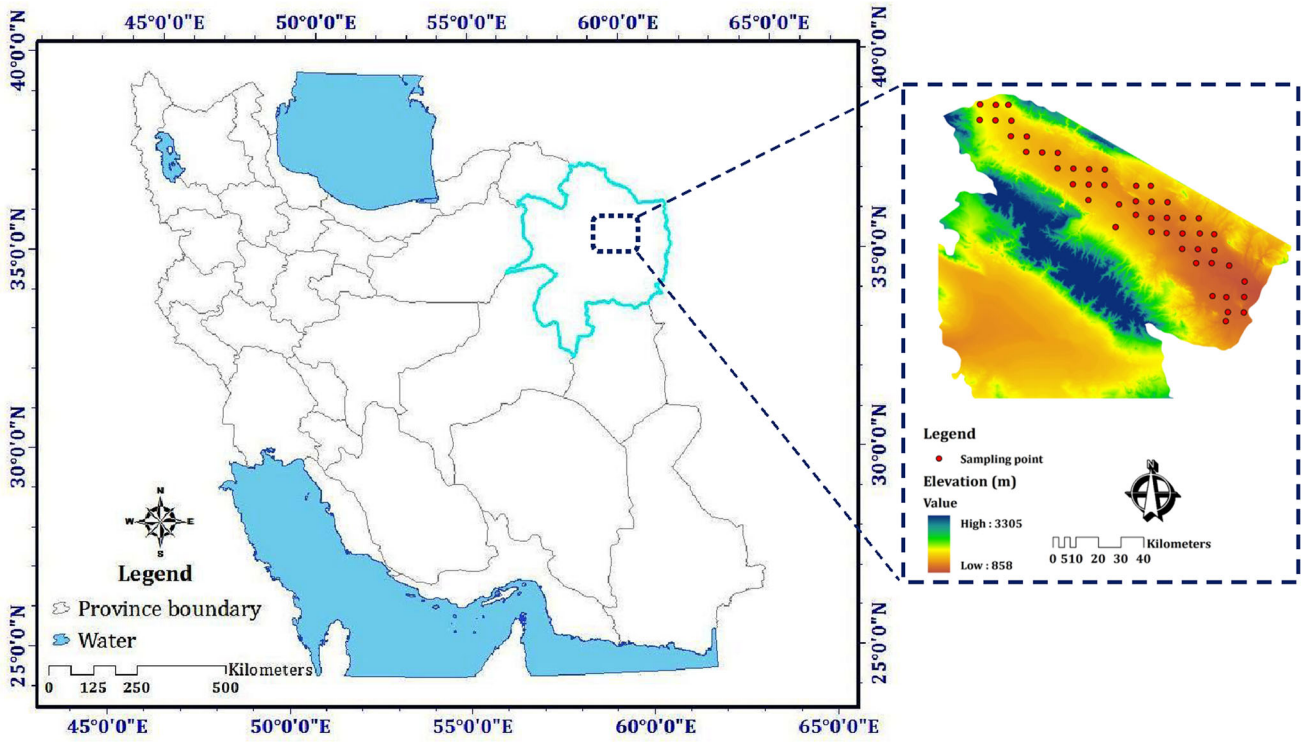

Fig. 3 Location and geographical position of the study area

Table 1 Descriptive statistics of data sets utilized for training and testing

Variable	Minimum	Maximum	Mean	SD	Range	Correlation with ESP
Training data						
EC_e (dS m^{-1})	0.01	16.00	2.11	2.38	15.99	0.825**
Clay (%)	4.00	41.00	19.21	7.43	37.00	0.267**
pH	7.70	8.40	8.10	0.12	0.70	−0.309**
ESP (%)	0.28	23.08	4.96	4.52	22.80	1
Testing data						
EC_e (dS m^{-1})	0.04	15.84	2.05	2.42	15.80	0.836**
Clay (%)	6.00	39.00	19.15	7.51	33.00	0.275**
pH	7.74	8.36	8.07	0.14	0.62	−0.302**
ESP (%)	0.31	15.00	4.80	4.47	14.69	1

SD standard deviation

** Significant at 0.01 level

Data collection, field sampling and laboratory analysis

Utilizing the stratified random sampling, 100 soil samples were collected from 0 to 30 and 30 to 60 cm depth. The collected soil samples were air dried, crushed and sieved using a 2 mm sieve size and subsequently subjected to analysis. The laboratory tests on the soil samples, including particle size distribution (i.e., clay, silt and sand fractions) and measurement of soil EC_e (EC of saturated soil paste extract) and pH were performed in accordance with Sparks et al. (1996). Before selection of inputs and output variable, data points were tested through Kolmogorov–Smirnov test. Outliers were separated and data normality was confirmed. After data processing and outlier elimination, the data number reduced to 98 points, which were processed further using the MLP and ANFIS models. Data points were randomized by Excel software and 65 % of the data was applied as training data, while remaining 20 and 15 % were utilized as a test and validation data, respectively. The cross validation technique (Fijani et al. 2013; Barzegar et al. 2016a, b) was utilized to divide the data set. Data

points were standardized for equalization before the models training, which prevents excessive shrinking weights. The data points were converted between 0 and 1 numbers for most of the output threshold functions were found within this range. In order to cover all possible ranges of the data pattern, data division was carried out randomly, as mentioned before. The applied data were then normalized using the following equation to fix them between (0, 1):

$$y_{normal} = (y_0 - y_{min})/(y_{max} - y_{min}) \quad (11)$$

where, y_{max} and y_{min} represent the maximum and minimum values of each record, and y_0 shows the observed (recorded) values. Some descriptive statistics including minimum and maximum values, mean values, standard deviation (SD) and the range of the data utilized as well as the correlation coefficient between the ESP and the considered input variables for both training and testing data sets are listed in Table 1.

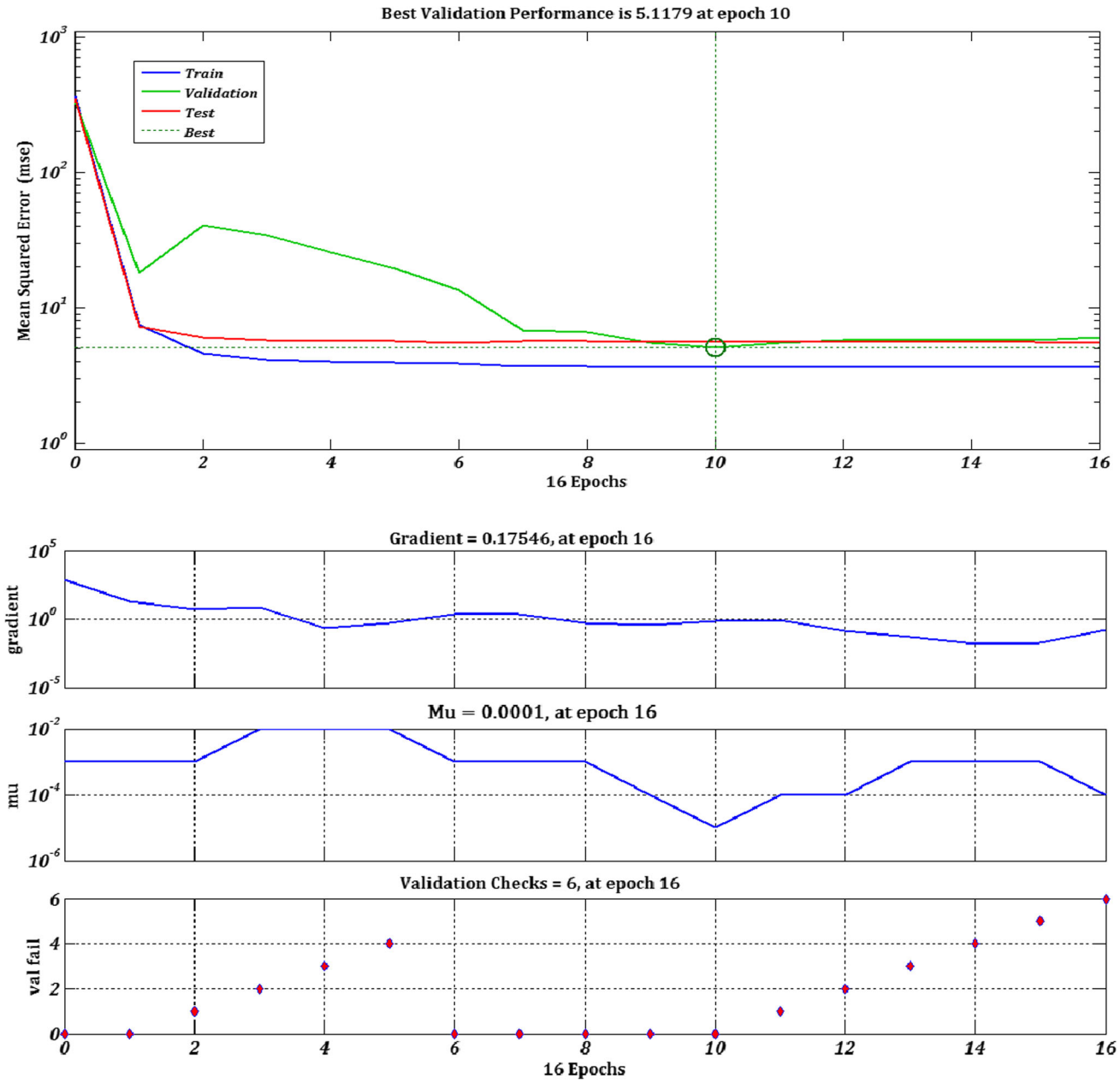

Fig. 4 Training state and performance of the developed MLP neural network model for prediction of ESP (%)

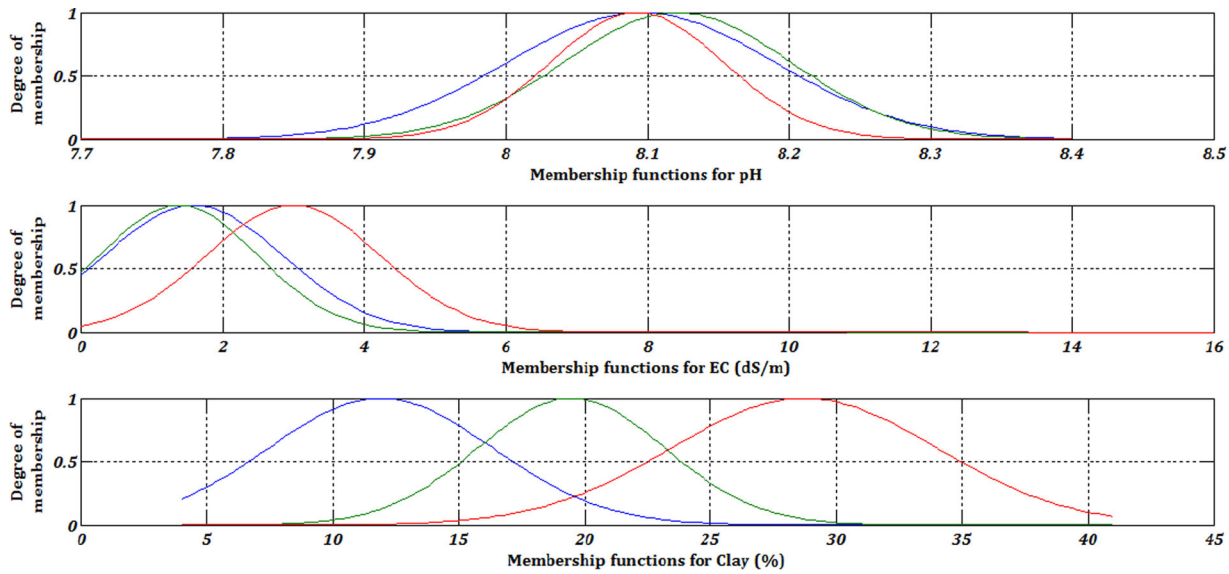

Fig. 5 Sugeno-FIS generated Gaussian membership functions for input variables of the ANFIS model

Model development

MLP model

To build up a three-layered ANN model, three inputs, including EC_e (dS m^{-1}), clay (%) and pH were used in the first layer and the ESP (%) as output was utilized in the last layer. The feed-forward neural network was trained with Levenberg–Marquardt algorithm (trainlm). The number of hidden neurons in MLP models was chosen via a trial and error method (Belayneh et al. 2014, 2016; Adamowski and Sun 2010; Barzegar et al. 2016a, b). However, Wanas et al. (1998) and Mishra and Desai (2006) empirically considered the equations, e.g. log (N), where N is the number of training samples and $2n + 1$, where n is the number of input neurons to determine the number of hidden neurons. In this study, the optimal number of hidden neurons was determined to be between log (N) and $(2n + 1)$. By utilizing the Wanas et al. (1998) method, two hidden neurons and by using the Mishra and Desai (2006) method, seven hidden neurons were considered; thereafter the optimal number was chosen via trial and error. The number of neurons in the hidden layer was 3.

TANSIG and PURELIN functions were utilized as the transfer functions in the hidden layer. The performance plot (Fig. 4) demonstrates the value of the function, in terms of training, validation, and testing behaviors, versus the iteration number. The best validation performance was at epoch 10 based on the mean square error equal to 5.1179. The magnitude of the gradient and the number of validation checks used to terminate network training are illustrated in Fig. 4. At an epoch of 16 iterations, the gradient was 0.17546, barely above the 1×10^{-1} threshold below, which training will stop, and at six, the validation checks indicated training should stop. When the training of the model was completed, the testing data set serves as model input and ESP values were predicted.

ANFIS model

To build up the ANFIS model, hybrid algorithm which is the combination of the least-squares method and the back propagation gradient descent method was applied to optimize and adjust the Gaussian membership function parameters and coefficients of the output linear equations (Zounemat-Kermani and Teshnehlab 2008; Fijani et al. 2013). In this study, the Gaussian membership function was used because it generated the least error in the fuzzification of the data collected for the components. The number of epochs and error tolerance were set to 500 and 0, respectively. Fuzzy subtractive clustering, based on a measure of the density of data points in the feature space (Chiu 1994), was used to establish the rule-based relationship between the input

Table 2 The results of the proposed models in the training and testing steps for prediction of ESP (%)

Model	Training step		Testing step	
	R^2	MSE (%)	R^2	MSE (%)
MLP	0.9099	5.0184	0.8429	5.3611
ANFIS	0.9236	4.7120	0.8964	5.0935

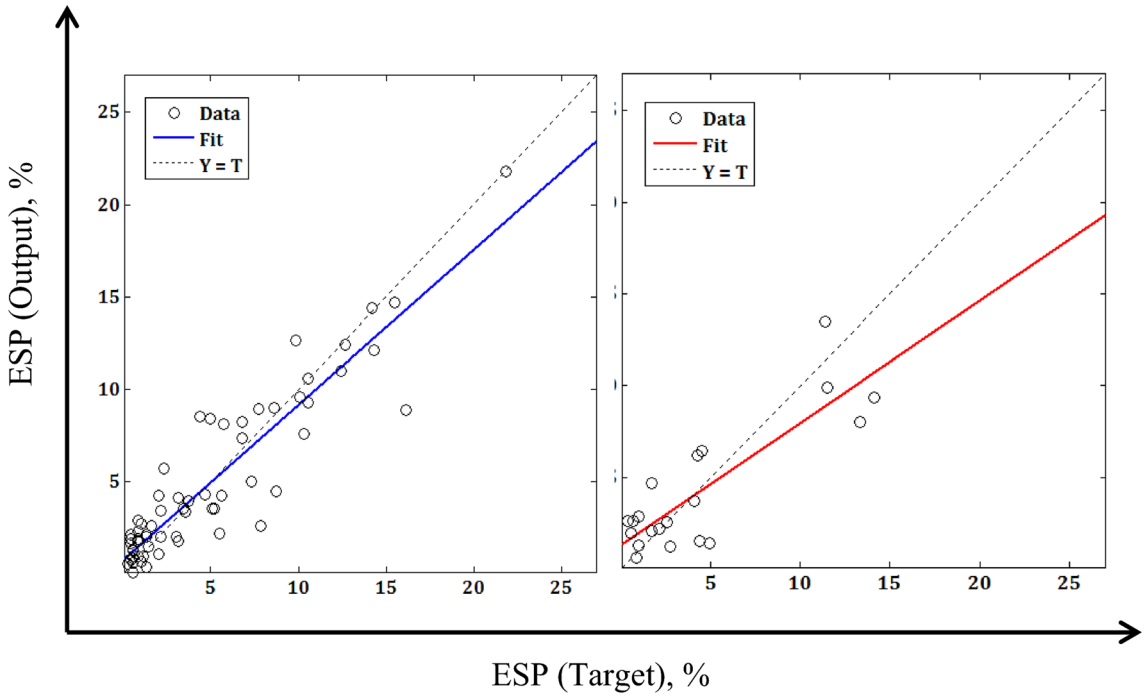

Fig. 6 Scatter plots of target versus output in training (*left*) and testing (*right*) steps for MLP model

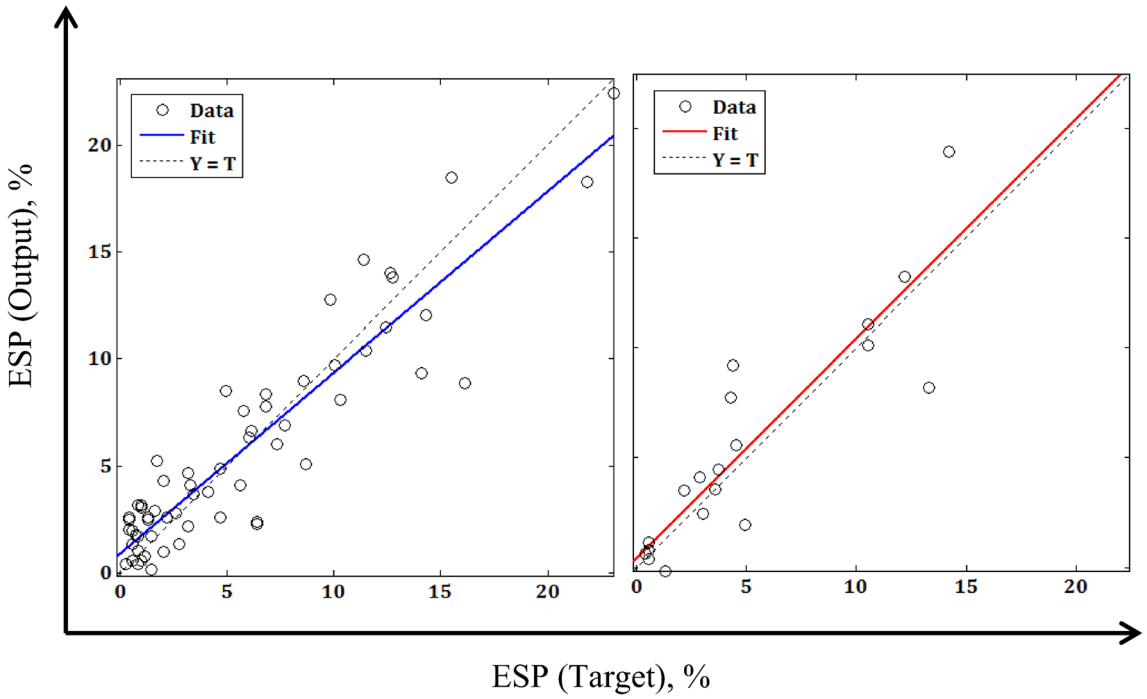

Fig. 7 Scatter plots of target versus output in training (*left*) and testing (*right*) steps for ANFIS model

and output variables. The best ANFIS model performance was achieved after 100 epochs of training when the clustering radius was set to 0.5. Three Gaussian membership functions were extracted for the input variables of the ANFIS model (Fig. 5).

Results and discussion

The performance of MLP and ANFIS models was compared in this part of the study. After training the proposed model, the models were tested with 20 testing samples. The

results of the developed models in the training and testing steps are presented in Table 2. Figures 6 and 7 demonstrate the scatter plots of the target versus output in training and testing steps for MLP and ANFIS models.

Both of the models for the prediction of ESP revealed satisfactory results in terms of the statistical performance criteria. Therefore, these models were acceptable for prediction of ESP in the Mashhad plain, Northeast Iran. The proposed models obtained relatively lower prediction errors in training step as compared to the testing step indicated that these models exhibited relatively better generalization as compared to the prediction. The R^2 and MSE values of the MLP model in training step were 0.9099 and 5.0184 percent, respectively, whereas those were 0.8429 and 5.3611 percent, in the testing step. In the training step, the ANFIS model resulted in the R^2 of 0.9236 and MSE of 4.7120 percent, whereas, for the testing data, the corresponding values were 0.8964 and 5.0935 percent, respectively. The ANFIS model performance was slightly better than the MLP model. This result concurs with the studies of Barzegar et al. (2016a, b), Rajaee et al. (2009), Adamowski and Chan (2011), Nourani et al. (2011), Moosavi et al. (2013), Fijani et al. (2013), Emamgholizadeh et al. (2014) and Parmar and Bhardwaj (2015). This may be related to the effect of fuzzification of the input through membership functions (Barzegar et al. 2016a, b). It was concluded that the ANFIS model outperformed another developed model and this result was related to dimensional independence, global optimum and higher generalization capability of the ANFIS.

Conclusions

In the present study, two AI models including Multi-layer Perceptron (MLP) and Adaptive Neuro-Fuzzy Inference System (ANFIS) were assessed for the prediction of soil Exchangeable Sodium Percentage (ESP) in the Mashhad plain, Northeast Iran based on EC_e (dS m^{-1}), Clay (%) and pH. The coefficient of determination (R^2) and mean square error (MSE) were utilized to evaluate the model's performance. The R^2 and MSE values of the MLP model in testing step were 0.8429 and 5.3611 percent, respectively, whereas those were 0.8964 and 5.0935 percent, respectively for the ANFIS model. The ANFIS model outperformed the MLP model in the prediction of ESP values based on performance criteria. This was attributed to the effect of fuzzification of the input through membership functions.

References

Abdulshahed AM, Longstaff AP, Fletcher S (2015) The application of ANFIS prediction models for thermal error compensation on CNC machine tools. Appl Soft Comput 27:158–168

Adamowski JF, Chan HG (2011) A wavelet neural network conjunction model for groundwater level forecasting. J Hydrol 407(1–4):28–40

Adamowski JF, Sun K (2010) Development of a coupled wavelet transform and neural network method for flow forecasting of non-perennial rivers in semi-arid watersheds. J Hydrol 390(1–2):85–91

Adhikari P, Shukla MK, Mexal JG (2011) Spatial variability of electrical conductivity of desert soil irrigated with treated wastewater: implications for irrigation management. Appl Environ Soil 2011:1–11

Al-Busaidi AS, Cookson P (2003) Salinity-pH relationships in calcareous soils. Agric Mar Sci 8:41–46

Auerswald K, Simon S, Stanjek H (2001) Influence of soil properties on electrical conductivity under humid water regimes. Soil Sci 166:382–390

Ayers RS, Westcot DW (1989) Water quality for agriculture. FAO Irrigation and Drainage. Paper no 29, pp 1–174. Rome

Banaei MH, Moameni A, Bybordi M, Malakouti MJ (2005) The soil of Iran: new achievements in perception, management and use. SANA Publishing, Tehran **(In Persian)**

Barzegar R, Asghari Moghaddam A (2016) Combining the advantages of neural networks using the concept of committee machine in the groundwater salinity prediction. Model Earth Syst Environ. doi:10.1007/s40808-015-0072-8

Barzegar R, Adamowski J, Moghaddam AA (2016a) Application of wavelet-artificial intelligence hybrid models for water quality prediction: a case study in Aji-Chay River, Iran. Stoch Environ Res Risk Assess. doi:10.1007/s00477-016-1213-y

Barzegar R, Asghari Moghaddam A, Baghban H (2016b) A supervised committee machine artificial intelligent for improving DRASTIC method to assess groundwater contamination risk: a case study from Tabriz plain aquifer, Iran. Stoch Environ Res Risk Assess 30(3):883–899

Barzegar R, Sattarpour M, Nikudel MR, Asghari Moghaddam A (2016c) Comparative evaluation of artificial intelligence models for prediction of uniaxial compressive strength of travertine rocks, Case study: Azarshahr area, NW Iran. Model Earth Syst Environ. doi:10.1007/s40808-016-0132-8

Belayneh A, Adamowski J, Khalil B, Ozga-Zielinski B (2014) Long-term SPI drought forecasting in the Awash River Basin in Ethiopia using wavelet-support vector regression models. J Hydrol 508:418–429

Belayneh A, Adamowski J, Khalil B, Quilty J (2016) Coupling machine learning methods with wavelet transforms and the bootstrap and boosting ensemble approaches for drought. Atmos Res 172–173(15):37–47

Bohn HL, Mcneal BL, O'Connor GA (1985) Soil chemistry. Wiley, New York

Chiu S (1994) Fuzzy model identification based on cluster estimation. J Intell Fuzzy Syst 2:267–278

Emamgholizadeh S, Kashi H, Marofpoor I, Zalaghi E (2014) Prediction of water quality parameters of Karoon River (Iran) by artificial intelligence-based models. Int J Environ Sci Technol 11(3):645–656

Farahmand A, Oustan SH, Jafarzadeh AJ, Asgharzad A (2012) Salinity and sodicity parameters in some salt-affected soils of the Tabriz plain. Water Soil Sci (Agric Sci) 22:1–15

Fijani E, Nadiri AA, Asghari Moghaddam A, Tsai F, Dixon B (2013) Optimization of DRASTIC method by supervised committee machine artificial intelligence to assess groundwater vulnerability for Maragheh-Bonab plain aquifer Iran. J Hydrol 530:89–100

Haykin S (1999) Neural networks: a comprehensive foundation. Prentice-Hall, New Jersey, p 842

Jang JSR (1993) ANFIS: adaptive network based fuzzy inference system. IEEE Trans Syst Man Cybern 23(3):665–685

Keshavarzi A, Sarmadian F (2012) Mapping of spatial distribution of soil salinity and alkalinity in a semi-arid region. Ann Warsaw Agricult Univ SGGW Land Reclam 44(1):3–14

Kilic K, Kilic S (2007) Spatial variability of salinity and alkalinity of a field having salination risk in semi-arid climate in northern Turkey. Environ Monit Assess 127:55–65

Kisi O, Tombul M, Zounemat Kermani M (2015) Modeling soil temperatures at different depths by using three different neural computing techniques. Theor Appl Climatol 121(1):377–387

Malekmohammadi I, Bazargan-Lari MR, Kerachian R, Nikoo MR, Fallahnia M (2011) Evaluating the efficacy of SVMs, BNs, ANNs and ANFIS in wave height prediction. Ocean Eng 38:487–497

Mishra AK, Desai VR (2006) Drought forecasting using feed-forward recursive neural network. Ecol Model 198(1–2):127–138

Moosavi V, Vafakhah M, Shirmohammadi B, Behnia N (2013) A wavelet-ANFIS hybrid model for groundwater level forecasting for different prediction periods. Water Resour Manag 27(5):1301–1321

Nourani V, Kisi Z, Mehdi K (2011) Two hybrid artificial Intelligence approaches for modeling rainfall-runoff process. J Hydrol 402(1–2):41–59

Nourani V, Baghanam AH, Adamowski J, Gebremichael M (2013) Using self-organizing maps and wavelet transforms for space-time pre-processing of satellite precipitation and runoff data in neural network based rainfall-runoff modeling. J Hydrol 476:228–243

Omran EE (2008) Is soil science dead and buried? Future image in the world of 10 billion people. CATRINA 3(2):59–68

Parmar KS, Bhardwaj R (2015) River water prediction modeling using neural networks, fuzzy and wavelet coupled model. Water Resour Manag 29(1):17–33

Pessarakli M (1991) Dry matter yield, nitrogen-15 absorption, and water uptake by green bean under sodium chloride stress. J Crop Sci 31:1633–1640

Postel R (1989) Water of agriculture: facing the limits, world watch paper. World Watch Institute, Washington D.C

Pozdnyakova L, Zhang R (1999) Geostatistical analyses of soil salinity in a large field. Precis Agric 1:153–165

Rajaee T, Mirbagheri SA, Zounemat-Kermani M, Nourani V (2009) Daily suspended sediment concentration simulation using ANN and neuro-fuzzy models. Sci Total Environ 407(17):4916–4927

Rashidi M, Seilsepour M (2008) Modelling of soil cation exchange capacity based on some soil physical and chemical properties. ARPN J Agric Biol Sci 3:6–13

Robbins CW (1993) Coefficients for estimating SAR from soil pH and EC data and calculating pH from SAR and EC values in salinity models. Arid Soil Res Rehabil 7:29–38

Robbins CW, Meyer WS (1990) Calculating pH from EC and SAR values in salinity models and SAR from soil and bore water pH and EC data. Aust J Soil Res 28:1001–1011

Sarani F, Ahangar AGh, Shabani A (2015) Predicting ESP and SAR by artificial neural network and regression models using soil pH and EC data (Mi ankangi Region, Sistan and Baluchestan Province, Iran). Arch Agron Soil Sci 62(1):127–138

Seilsepour M, Rashidi M (2008a) Modelling of soil sodium adsorption ratio based on soil electrical conductivity. ARPN J Agric Biol Sci 3:27–31

Seilsepour M, Rashidi M (2008b) Prediction of soil cation exchange capacity based on some soil physical and chemical properties. World Appl Sci 3:200–205

Seilsepour M, Rashidi M (2008c) Modelling of soil cation exchange capacity based on soil colloidal matrix. American-Eurasian. J Agric Environ Sci 3:365–369

Sparks DL, Page AL, Helmke PA, Leoppert RH, Soltanpour PN, Tabatabai MA, Johnston GT, Summer ME (1996) Methods of soil analysis. Soil Science Society of America, Madison, Wisconsin

Wanas N, Auda G, Kamel MS, Karray F (1998) On the optimal number of hidden nodes in a neural network. In: Proceedings of the IEEE Canadian conference on electrical and computer engineering, vol 2, pp 918–921

Zounemat-Kermani M, Teshnehlab M (2008) Using adaptive neuro-fuzzy inference system for hydrological time series prediction. Appl Soft Comput 8(2):928–936